Evidence for an Excess of $\bar{B} \to D^{(*)}\tau^-\bar{\nu}_\tau$ Decays

J. P. Lees,[1] V. Poireau,[1] V. Tisserand,[1] J. Garra Tico,[2] E. Grauges,[2] A. Palano,[3b,3a] G. Eigen,[4] B. Stugu,[4] D. N. Brown,[5] L. T. Kerth,[5] Yu. G. Kolomensky,[5] G. Lynch,[5] H. Koch,[5] T. Schroeder,[6] D. J. Asgeirsson,[7] C. Hearty,[7] T. S. Mattison,[7] J. A. McKenna,[7] R. Y. So,[7] A. Khan,[8] V. E. Blinov,[9] A. R. Buzykaev,[9] V. P. Druzhinin,[9] V. B. Golubev,[9] E. A. Kravchenko,[9] A. P. Onuchin,[9] S. I. Serednyakov,[9] Yu. I. Skovpen,[9] E. P. Solodov,[9] K. Yu. Todyshev,[9] A. N. Yushkov,[9] M. Bondioli,[10] D. Kirkby,[10] A. J. Lankford,[10] M. Mandelkern,[10] H. Atmacan,[11] J. W. Gary,[11] F. Liu,[11] O. Long,[11] G. M. Vitug,[11] C. Campagnari,[12] T. M. Hong,[12] D. Kovalskyi,[12] J. D. Richman,[12] C. A. West,[12] A. M. Eisner,[13] J. Kroseberg,[13] W. S. Lockman,[13] A. J. Martinez,[13] B. A. Schumm,[13] A. Seiden,[13] D. S. Chao,[14] C. H. Cheng,[14] B. Echenard,[14] K. T. Flood,[14] D. G. Hitlin,[14] P. Ongmongkolkul,[14] F. C. Porter,[14] A. Y. Rakitin,[14] R. Andreassen,[15] Z. Huard,[15] B. T. Meadows,[15] M. D. Sokoloff,[15] L. Sun,[15] P. C. Bloom,[16] W. T. Ford,[16] A. Gaz,[16] U. Nauenberg,[16] J. G. Smith,[16] S. R. Wagner,[16] R. Ayad,[17,*] W. H. Toki,[17] B. Spaan,[18] K. R. Schubert,[19] R. Schwierz,[19] D. Bernard,[20] M. Verderi,[20] P. J. Clark,[21] S. Playfer,[21] D. Bettoni,[22a] C. Bozzi,[22a] R. Calabrese,[22b,22a] G. Cibinetto,[22b,22a] E. Fioravanti,[22b,22a] I. Garzia,[22b,22a] E. Luppi,[22b,22a] M. Munerato,[22b,22a] L. Piemontese,[22a] V. Santoro,[22a] R. Baldini-Ferroli,[23] A. Calcaterra,[23] R. de Sangro,[23] G. Finocchiaro,[23] P. Patteri,[23] I. M. Peruzzi,[23,†] M. Piccolo,[23] M. Rama,[23] A. Zallo,[23] R. Contri,[24b,24a] E. Guido,[24b,24a] M. Lo Vetere,[24b,24a] M. R. Monge,[24b,24a] S. Passaggio,[24a] C. Patrignani,[24b,24a] E. Robutti,[24a] B. Bhuyan,[25] V. Prasad,[25] C. L. Lee,[26] M. Morii,[26] A. J. Edwards,[27] A. Adametz,[28] U. Uwer,[28] H. M. Lacker,[29] T. Lueck,[29] P. D. Dauncey,[30] U. Mallik,[31] C. Chen,[32] J. Cochran,[32] W. T. Meyer,[32] S. Prell,[32] A. E. Rubin,[32] A. V. Gritsan,[33] Z. J. Guo,[33] N. Arnaud,[34] M. Davier,[34] D. Derkach,[34] G. Grosdidier,[34] F. Le Diberder,[34] A. M. Lutz,[34] B. Malaescu,[34] P. Roudeau,[34] M. H. Schune,[34] A. Stocchi,[34] G. Wormser,[34] D. J. Lange,[35] D. M. Wright,[35] C. A. Chavez,[36] J. P. Coleman,[36] J. R. Fry,[36] E. Gabathuler,[36] D. E. Hutchcroft,[36] D. J. Payne,[36] C. Touramanis,[36] A. J. Bevan,[37] F. Di Lodovico,[37] R. Sacco,[37] M. Sigamani,[37] G. Cowan,[38] D. N. Brown,[39] C. L. Davis,[39] A. G. Denig,[40] M. Fritsch,[40] W. Gradl,[40] K. Griessinger,[40] A. Hafner,[40] E. Prencipe,[40] R. J. Barlow,[41,‡] G. Jackson,[41] G. D. Lafferty,[41] E. Behn,[42] R. Cenci,[42] B. Hamilton,[42] A. Jawahery,[42] D. A. Roberts,[42] C. Dallapiccola,[43] R. Cowan,[44] D. Dujmic,[44] G. Sciolla,[44] R. Cheaib,[45] D. Lindemann,[45] P. M. Patel,[45] S. H. Robertson,[45] P. Biassoni,[46b,46a] N. Neri,[46a] F. Palombo,[46b,46a] S. Stracka,[46b,46a] L. Cremaldi,[47] R. Godang,[47,§] R. Kroeger,[47] P. Sonnek,[47] D. J. Summers,[47] X. Nguyen,[48] M. Simard,[48] P. Taras,[48] G. De Nardo,[49b,49a] D. Monorchio,[49b,49a] G. Onorato,[49b,49a] C. Sciacca,[49b,49a] M. Martinelli,[50] G. Raven,[50] C. P. Jessop,[51] J. M. LoSecco,[51] W. F. Wang,[51] K. Honscheid,[52] R. Kass,[52] J. Brau,[53] R. Frey,[53] N. B. Sinev,[53] D. Strom,[53] E. Torrence,[53] E. Feltresi,[54b,54a] N. Gagliardi,[54b,54a] M. Margoni,[54b,54a] M. Morandin,[54a] M. Posocco,[54a] M. Rotondo,[54a] G. Simi,[54a] F. Simonetto,[54b,54a] R. Stroili,[54b,54a] S. Akar,[55] E. Ben-Haim,[55] M. Bomben,[55] G. R. Bonneaud,[55] H. Briand,[55] G. Calderini,[55] J. Chauveau,[55] O. Hamon,[55] Ph. Leruste,[55] G. Marchiori,[55] J. Ocariz,[55] S. Sitt,[56b,56a] M. Biasini,[56b,56a] E. Manoni,[56b,56a] S. Pacetti,[56b,56a] A. Rossi,[56b,56a] C. Angelini,[57b,57a] G. Batignani,[57b,57a] S. Bettarini,[57b,57a] M. Carpinelli,[57b,57a,‖] G. Casarosa,[57b,57a] A. Cervelli,[57b,57a] F. Forti,[57b,57a] M. A. Giorgi,[57b,57a] A. Lusiani,[57c,57a] B. Oberhof,[57b,57a] E. Paoloni,[57b,57a] A. Perez,[57a] G. Rizzo,[57b,57a] J. J. Walsh,[57a] D. Lopes Pegna,[58] J. Olsen,[58] A. J. S. Smith,[58] A. V. Telnov,[58] F. Anulli,[59a] R. Faccini,[59a] F. Ferrarotto,[59a] F. Ferroni,[59b,59a] M. Gaspero,[59b,59a] L. Li Gioi,[59a] M. A. Mazzoni,[59a] G. Piredda,[59a] C. Bünger,[60] O. Grünberg,[60] T. Hartmann,[60] T. Leddig,[60] H. Schröder,[60,¶] C. Voss,[60] R. Waldi,[60] T. Adye,[61] E. O. Olaiya,[61] F. F. Wilson,[61] S. Emery,[62] G. Hamel de Monchenault,[62] G. Vasseur,[62] Ch. Yèche,[62] D. Aston,[63] D. J. Bard,[63] R. Bartoldus,[63] J. F. Benitez,[63] C. Cartaro,[63] M. R. Convery,[63] J. Dorfan,[63] G. P. Dubois-Felsmann,[63] W. Dunwoodie,[63] M. Ebert,[63] R. C. Field,[63] M. Franco Sevilla,[63] B. G. Fulsom,[63] A. M. Gabareen,[63] M. T. Graham,[63] P. Grenier,[63] C. Hast,[63] W. R. Innes,[63] M. H. Kelsey,[63] P. Kim,[63] M. L. Kocian,[63] D. W. G. S. Leith,[63] P. Lewis,[63] B. Lindquist,[63] S. Luitz,[63] V. Luth,[63] H. L. Lynch,[63] D. B. MacFarlane,[63] D. R. Muller,[63] H. Neal,[63] S. Nelson,[63] M. Perl,[63] T. Pulliam,[63] B. N. Ratcliff,[63] A. Roodman,[63] A. A. Salnikov,[63] R. H. Schindler,[63] A. Snyder,[63] D. Su,[63] M. K. Sullivan,[63] J. Va'vra,[63] A. P. Wagner,[63] W. J. Wisniewski,[63] M. Wittgen,[63] D. H. Wright,[63] H. W. Wulsin,[63] C. C. Young,[63] V. Ziegler,[63] W. Park,[64] M. V. Purohit,[64] R. M. White,[64] J. R. Wilson,[64] A. Randle-Conde,[65] S. J. Sekula,[65] M. Bellis,[66] P. R. Burchat,[66] T. S. Miyashita,[66] E. M. T. Puccio,[66] M. S. Alam,[67] J. A. Ernst,[67] R. Gorodeisky,[68] N. Guttman,[68] D. R. Peimer,[68] A. Soffer,[68] P. Lund,[69] S. M. Spanier,[69] J. L. Ritchie,[70] A. M. Ruland,[70] R. F. Schwitters,[70] B. C. Wray,[70] J. M. Izen,[71] X. C. Lou,[71] F. Bianchi,[72b,72a] D. Gamba,[72b,72a] S. Zambito,[72b,72a] L. Lanceri,[73b,73a] L. Vitale,[73b,73a] F. Martinez-Vidal,[74] A. Oyanguren,[74] H. Ahmed,[75] J. Albert,[75] Sw. Banerjee,[75] F. U. Bernlochner,[75] H. H. F. Choi,[75] G. J. King,[75] R. Kowalewski,[75] M. J. Lewczuk,[75] I. M. Nugent,[75] J. M. Roney,[75] R. J. Sobie,[75] N. Tasneem,[75] T. J. Gershon,[1] P. F. Harrison,[1] T. E. Latham,[1] H. R. Band,[77] S. Dasu,[77] Y. Pan,[77] R. Prepost,[77] and S. L. Wu[77]

(*BABAR* Collaboration)

[1]*Laboratoire d'Annecy-le-Vieux de Physique des Particules (LAPP), Université de Savoie, CNRS/IN2P3, F-74941 Annecy-Le-Vieux, France*
[2]*Universitat de Barcelona, Facultat de Fisica, Departament ECM, E-08028 Barcelona, Spain*
[3a]*INFN Sezione di Bari, I-70126 Bari, Italy*
[3b]*Dipartimento di Fisica, Università di Bari, I-70126 Bari, Italy*
[4]*University of Bergen, Institute of Physics, N-5007 Bergen, Norway*
[5]*Lawrence Berkeley National Laboratory and University of California, Berkeley, California 94720, USA*
[6]*Ruhr Universität Bochum, Institut für Experimentalphysik 1, D-44780 Bochum, Germany*
[7]*University of British Columbia, Vancouver, British Columbia, Canada V6T 1Z1*
[8]*Brunel University, Uxbridge, Middlesex UB8 3PH, United Kingdom*
[9]*Budker Institute of Nuclear Physics, Novosibirsk 630090, Russia*
[10]*University of California at Irvine, Irvine, California 92697, USA*
[11]*University of California at Riverside, Riverside, California 92521, USA*
[12]*University of California at Santa Barbara, Santa Barbara, California 93106, USA*
[13]*University of California at Santa Cruz, Institute for Particle Physics, Santa Cruz, California 95064, USA*
[14]*California Institute of Technology, Pasadena, California 91125, USA*
[15]*University of Cincinnati, Cincinnati, Ohio 45221, USA*
[16]*University of Colorado, Boulder, Colorado 80309, USA*
[17]*Colorado State University, Fort Collins, Colorado 80523, USA*
[18]*Technische Universität Dortmund, Fakultät Physik, D-44221 Dortmund, Germany*
[19]*Technische Universität Dresden, Institut für Kern- und Teilchenphysik, D-01062 Dresden, Germany*
[20]*Laboratoire Leprince-Ringuet, Ecole Polytechnique, CNRS/IN2P3, F-91128 Palaiseau, France*
[21]*University of Edinburgh, Edinburgh EH9 3JZ, United Kingdom*
[22a]*INFN Sezione di Ferrara, I-44100 Ferrara, Italy*
[22b]*Dipartimento di Fisica, Università di Ferrara, I-44100 Ferrara, Italy*
[23]*INFN Laboratori Nazionali di Frascati, I-00044 Frascati, Italy*
[24a]*INFN Sezione di Genova, I-16146 Genova, Italy*
[24b]*Dipartimento di Fisica, Università di Genova, I-16146 Genova, Italy*
[25]*Indian Institute of Technology Guwahati, Guwahati, Assam, 781 039, India*
[26]*Harvard University, Cambridge, Massachusetts 02138, USA*
[27]*Harvey Mudd College, Claremont, California 91711, USA*
[28]*Universität Heidelberg, Physikalisches Institut, Philosophenweg 12, D-69120 Heidelberg, Germany*
[29]*Humboldt-Universität zu Berlin, Institut für Physik, Newtonstrasse 15, D-12489 Berlin, Germany*
[30]*Imperial College London, London, SW7 2AZ, United Kingdom*
[31]*University of Iowa, Iowa City, Iowa 52242, USA*
[32]*Iowa State University, Ames, Iowa 50011-3160, USA*
[33]*Johns Hopkins University, Baltimore, Maryland 21218, USA*
[34]*Laboratoire de l'Accélérateur Linéaire, IN2P3/CNRS et Université Paris-Sud 11, Centre Scientifique d'Orsay, B.P. 34, F-91898 Orsay Cedex, France*
[35]*Lawrence Livermore National Laboratory, Livermore, California 94550, USA*
[36]*University of Liverpool, Liverpool L69 7ZE, United Kingdom*
[37]*Queen Mary, University of London, London, E1 4NS, United Kingdom*
[38]*University of London, Royal Holloway and Bedford New College, Egham, Surrey TW20 0EX, United Kingdom*
[39]*University of Louisville, Louisville, Kentucky 40292, USA*
[40]*Johannes Gutenberg-Universität Mainz, Institut für Kernphysik, D-55099 Mainz, Germany*
[41]*University of Manchester, Manchester M13 9PL, United Kingdom*
[42]*University of Maryland, College Park, Maryland 20742, USA*
[43]*University of Massachusetts, Amherst, Massachusetts 01003, USA*
[44]*Massachusetts Institute of Technology, Laboratory for Nuclear Science, Cambridge, Massachusetts 02139, USA*
[45]*McGill University, Montréal, Québec, Canada H3A 2T8*
[46a]*INFN Sezione di Milano, I-20133 Milano, Italy*
[46b]*Dipartimento di Fisica, Università di Milano, I-20133 Milano, Italy*
[47]*University of Mississippi, University, Mississippi 38677, USA*
[48]*Université de Montréal, Physique des Particules, Montréal, Québec, Canada H3C 3J7*
[49a]*INFN Sezione di Napoli, I-80126 Napoli, Italy*
[49b]*Dipartimento di Scienze Fisiche, Università di Napoli Federico II, I-80126 Napoli, Italy*
[50]*NIKHEF, National Institute for Nuclear Physics and High Energy Physics, NL-1009 DB Amsterdam, Netherlands*

[51]University of Notre Dame, Notre Dame, Indiana 46556, USA
[52]Ohio State University, Columbus, Ohio 43210, USA
[53]University of Oregon, Eugene, Oregon 97403, USA
[54a]INFN Sezione di Padova, I-35131 Padova, Italy
[54b]Dipartimento di Fisica, Università di Padova, I-35131 Padova, Italy
[55]Laboratoire de Physique Nucléaire et de Hautes Energies, IN2P3/CNRS, Université Pierre et Marie Curie-Paris6, Université Denis Diderot-Paris7, F-75252 Paris, France
[56a]INFN Sezione di Perugia, I-06100 Perugia, Italy
[56b]Dipartimento di Fisica, Università di Perugia, I-06100 Perugia, Italy
[57a]INFN Sezione di Pisa, I-56127 Pisa, Italy
[57b]Dipartimento di Fisica, Università di Pisa, I-56127 Pisa, Italy
[57c]Scuola Normale Superiore di Pisa, I-56127 Pisa, Italy
[58]Princeton University, Princeton, New Jersey 08544, USA
[59a]INFN Sezione di Roma, I-00185 Roma, Italy
[59b]Dipartimento di Fisica, Università di Roma La Sapienza, I-00185 Roma, Italy
[60]Universität Rostock, D-18051 Rostock, Germany
[61]Rutherford Appleton Laboratory, Chilton, Didcot, Oxon, OX11 0QX, United Kingdom
[62]CEA, Irfu, SPP, Centre de Saclay, F-91191 Gif-sur-Yvette, France
[63]SLAC National Accelerator Laboratory, Stanford, California 94309, USA
[64]University of South Carolina, Columbia, South Carolina 29208, USA
[65]Southern Methodist University, Dallas, Texas 75275, USA
[66]Stanford University, Stanford, California 94305-4060, USA
[67]State University of New York, Albany, New York 12222, USA
[68]Tel Aviv University, School of Physics and Astronomy, Tel Aviv, 69978, Israel
[69]University of Tennessee, Knoxville, Tennessee 37996, USA
[70]University of Texas at Austin, Austin, Texas 78712, USA
[71]University of Texas at Dallas, Richardson, Texas 75083, USA
[72a]INFN Sezione di Torino, I-10125 Torino, Italy
[72b]Dipartimento di Fisica Sperimentale, Università di Torino, I-10125 Torino, Italy
[73a]INFN Sezione di Trieste, I-34127 Trieste, Italy
[73b]Dipartimento di Fisica, Università di Trieste, I-34127 Trieste, Italy
[74]IFIC, Universitat de Valencia-CSIC, E-46071 Valencia, Spain
[75]University of Victoria, Victoria, British Columbia, Canada V8W 3P6
[1]Department of Physics, University of Warwick, Coventry CV4 7AL, United Kingdom
[77]University of Wisconsin, Madison, Wisconsin 53706, USA
(Received 31 May 2012; published 6 September 2012)

Based on the full *BABAR* data sample, we report improved measurements of the ratios $\mathcal{R}(D^{(*)}) = \mathcal{B}(\bar{B} \to D^{(*)}\tau^-\bar{\nu}_\tau)/\mathcal{B}(\bar{B} \to D^{(*)}\ell^-_\ell\bar{\nu}_\ell)$, where ℓ is either e or μ. These ratios are sensitive to new physics contributions in the form of a charged Higgs boson. We measure $\mathcal{R}(D) = 0.440 \pm 0.058 \pm 0.042$ and $\mathcal{R}(D^*) = 0.332 \pm 0.024 \pm 0.018$, which exceed the standard model expectations by 2.0σ and 2.7σ, respectively. Taken together, our results disagree with these expectations at the 3.4σ level. This excess cannot be explained by a charged Higgs boson in the type II two-Higgs-doublet model.

DOI: 10.1103/PhysRevLett.109.101802 PACS numbers: 13.20.He, 14.40.Nd, 14.80.Da

In the standard model (SM), semileptonic decays of B mesons are well-understood processes mediated by a W boson [1–3]. Decays involving the higher mass τ lepton are sensitive to additional amplitudes, such as those involving an intermediate charged Higgs boson [4–8], and offer an excellent opportunity to search for this and other non-SM contributions.

Our understanding of exclusive semileptonic decays has greatly improved over the past two decades, thanks to the development of heavy-quark effective theory and precise measurements of $\bar{B} \to D^{(*)}\ell^-\bar{\nu}_\ell$ [9] at the B factories [10,11]. SM expectations for the relative rates $\mathcal{R}(D^{(*)}) = \mathcal{B}(\bar{B} \to D^{(*)}\tau^-\bar{\nu}_\tau)/\mathcal{B}(\bar{B} \to D^{(*)}\ell^-\bar{\nu}_\ell)$ have less than 6% uncertainty [8]. Calculations [4–8] based on two-Higgs-doublet models (2HDM) predict a substantial impact on the ratio $\mathcal{R}(D)$ and a smaller effect on $\mathcal{R}(D^*)$. The ratios $\mathcal{R}(D)$ and $\mathcal{R}(D^*)$ are independent of the Cabibbo-Kobayashi-Maskawa element $|V_{cb}|$ and also, to a large extent, of the parameterization of the hadronic matrix elements.

The decay $\bar{B} \to D^*\tau^-\bar{\nu}_\tau$ was first observed in 2007 by the Belle Collaboration [12]. Since then, both *BABAR* and Belle have published improved measurements and have found evidence for $\bar{B} \to D\tau^-\bar{\nu}_\tau$ decays [13–15]. Although the measured values for $\mathcal{R}(D)$ and $\mathcal{R}(D^*)$ have consistently exceeded the SM expectations, the significance

of the excess has remained low due to the large statistical uncertainties.

This analysis is an update of an earlier *BABAR* measurement [13]. It is based on the full *BABAR* data sample and includes improvements to the event reconstruction that increase the signal efficiency by more than a factor of 3.

We analyze data recorded with the *BABAR* detector [16] at a center-of-mass (c.m.) energy of 10.58 GeV, corresponding to the mass of the $\Upsilon(4S)$ resonance, which decays almost exclusively to $B\bar{B}$ pairs. The data sample comprises an integrated luminosity of 426 fb^{-1} and contains 471×10^6 $B\bar{B}$ pairs. An additional sample of 40 fb^{-1}, taken at a c.m. energy 40 MeV below the $\Upsilon(4S)$ resonance (off-peak data), is used to study continuum background from $e^+e^- \to f\bar{f}(\gamma)$ pair production with $f = u, d, s, c, \tau$.

We choose to reconstruct only the purely leptonic decays of the τ lepton, $\tau^- \to e^-\bar{\nu}_e\nu_\tau$ and $\tau^- \to e^-\bar{\nu}_\mu\nu_\tau$, so that $\bar{B} \to D^{(*)}\tau^-\bar{\nu}_\tau$ (signal) and $\bar{B} \to D^{(*)}\ell^-\bar{\nu}_\ell$ (normalization) events are identified by the same particles in the final state. This leads to the cancellation of various sources of uncertainty in the ratios $\mathcal{R}(D^{(*)})$. Events corresponding to $\Upsilon(4S) \to B\bar{B}$ decays are selected by reconstructing the hadronic decay of one of the B mesons ($B_{\rm tag}$), a $D^{(*)}$ meson, and a lepton (e or μ). Signal and normalization yields are extracted from a fit to the spectra of two variables: the invariant mass of the undetected particles $m^2_{\rm miss} = p^2_{\rm miss} = (p_{e^+e^-} - p_{\rm tag} - p_{D^{(*)}} - p_\ell)^2$ (where p denotes the four-momenta of the colliding beams, the $B_{\rm tag}$, the $D^{(*)}$, and the charged lepton) and the lepton three-momentum in the B rest frame $|\boldsymbol{p}^*_\ell|$. The $m^2_{\rm miss}$ distribution of decays with a single missing neutrino peaks at zero, whereas signal events, which have three missing neutrinos, have a broad $m^2_{\rm miss}$ distribution that extends to about 9 GeV^2. The observed lepton in signal events is a secondary particle from the τ decay, so its $|\boldsymbol{p}^*_\ell|$ spectrum is softer than for normalization events.

The $B_{\rm tag}$ reconstruction has been greatly improved with respect to previous analyses [17]. We now reconstruct $B_{\rm tag}$ candidates in 1680 final states. We look for decays of the type $B_{\rm tag} \to SX^\pm$, where S refers to a seed meson (D^0, D^{*0}, D^+, D^{*+}, D_s^+, D_s^{*+}, or J/ψ) reconstructed in 56 different decay modes and $X^\pm$ is a charged state decaying to up to five hadrons ($\pi^\pm$, $K^\pm$, π^0, and K^0_S). Two kinematic variables are used to select $B_{\rm tag}$ candidates: $m_{\rm ES} = \sqrt{E^2_{\rm beam} - \boldsymbol{p}^2_{\rm tag}}$ and $\Delta E = E_{\rm tag} - E_{\rm beam}$. Here $\boldsymbol{p}_{\rm tag}$ and $E_{\rm tag}$ refer to the c.m. momentum and energy of the $B_{\rm tag}$, and $E_{\rm beam}$ is the c.m. energy of a single beam particle. For correctly reconstructed B decays, the $m_{\rm ES}$ distribution is centered at the B-meson mass with a resolution of 2.5 MeV, while ΔE is centered at zero with a resolution of 18 MeV. We require $m_{\rm ES} > 5.27$ GeV and $|\Delta E| < 0.072$ GeV.

We combine each $B_{\rm tag}$ candidate with a $D^{(*)}$ meson candidate and a charged lepton ℓ. Events with additional charged particles are rejected. The laboratory momentum of the electron or muon is required to exceed 300 or 200 MeV, respectively. D decays are reconstructed in the following decay modes: $D^0 \to K^-\pi^+$, K^-K^+, $K^-\pi^+\pi^0$, $K^-\pi^+\pi^-\pi^+$, $K^0_S\pi^+\pi^-$; $D^+ \to K^-\pi^+\pi^+$, $K^-\pi^+\pi^+\pi^0$, $K^0_S\pi^+$, $K^0_S\pi^+\pi^+\pi^-$, $K^0_S\pi^+\pi^0$, $K^0_SK^+$, with $K^0_S \to \pi^+\pi^-$. For D^* candidates, the decays $D^{*+} \to D^0\pi^+$, $D^+\pi^0$, and $D^{*0} \to D^0\pi^0$, $D^0\gamma$ are used.

In events with more than one reconstructed $B\bar{B}$ pair, we select the candidate with the lowest value of $E_{\rm extra}$, defined as the sum of the energies of all photon candidates not associated with the reconstructed $B\bar{B}$ pair. We further reject combinatorial background and normalization events by requiring $q^2 = (p_B - p_{D^{(*)}})^2 > 4$ GeV^2 and $|\boldsymbol{p}_{\rm miss}| > 200$ MeV, where $|\boldsymbol{p}_{\rm miss}|$ is the missing momentum in the c.m. frame.

We divide the $B_{\rm tag}D^{(*)}\ell$ candidates that satisfy the previous requirements into eight subsamples: four $D^{(*)}\ell$ samples, one for each of the types of charm meson reconstructed ($D^0\ell$, $D^{*0}\ell$, $D^+\ell$, and $D^{*+}\ell$), and four $D^{(*)}\pi^0\ell$ control samples with the same selection plus an additional π^0. These control samples constrain the poorly understood $\bar{B} \to D^{**}(\ell/\tau)\nu$ background (where D^{**} refers to charm resonances heavier than the D^* ground state mesons), which enters the $D^{(*)}\ell$ sample predominantly when the π^0 from $D^{**} \to D^{(*)}\pi^0$ decays is not detected. The $D^{(*)}\pi^0\ell$ samples have a very large continuum background, so we restrict this sample to events with $|\cos\Delta\theta_{\rm thrust}| < 0.8$, where $\Delta\theta_{\rm thrust}$ is the angle between the thrust axes of the $B_{\rm tag}$ and of the rest of the event.

We improve the separation between well-reconstructed events (signal and normalization) and the various backgrounds by using boosted decision tree (BDT) selectors [18]. For each of the four $D^{(*)}\ell$ samples, we train a BDT to select signal and normalization events and reject $D^{**}\ell\bar{\nu}$ background and charge cross-feed, defined as $D^{(*)}(\ell/\tau)\nu$ decays reconstructed with the wrong charge. Each BDT selector relies on the simulated distributions of the following variables: (1) $E_{\rm extra}$; (2) ΔE; (3) the reconstructed mass of the signal D meson; (4) the mass difference for the reconstructed signal D^*: $\Delta m = m(D\pi) - m(D)$; (5) the reconstructed mass of the seed meson of the $B_{\rm tag}$; (6) the mass difference for a D^* originating from the $B_{\rm tag}$, $\Delta m_{\rm tag} = m(D_{\rm tag}\pi) - m(D_{\rm tag})$; (7) the charged particle multiplicity of the $B_{\rm tag}$ candidate; and (8) $\cos\Delta\theta_{\rm thrust}$. For the $D^{(*)}\pi^0\ell$ samples, we use similar BDT selectors that are trained to reject continuum, $D^{(*)}(\ell/\tau)\nu$, and other $B\bar{B}$ events. After the BDT requirements are applied, the fraction of events attributed to signal in the $m^2_{\rm miss} > 1.5$ GeV^2 region, which excludes most of the normalization decays, increases from 2% to 39%. The remaining background is composed of normalization events (10%), continuum (19%), $D^{**}(\ell/\tau)\nu$ events (13%), and other $B\bar{B}$ events (19%), primarily from $B \to D^{(*)}D_s^{(*)+}$ decays with $D_s^+ \to \tau^+\nu_\tau$.

As described below, the fit procedure relies on the Monte Carlo (MC) simulation [19–21] of the two-dimensional $m^2_{\rm miss} - |\boldsymbol{p}^*_\ell|$ spectra of the different signal and background contributions. For semileptonic decays, we parameterize the hadronic matrix elements of the signal and normalization decays by using heavy-quark effective theory-based form factors (FFs) [22]. For low-mass leptons, there is effectively one FF for $\bar{B} \to D\ell^-\bar{\nu}_\ell$, whereas there are three FFs for $\bar{B} \to D^*\ell^-\bar{\nu}_\ell$ decays, all of which have been measured with good precision [23]. For heavy leptons, each of these decays depends on an additional FF which can be calculated by using heavy-quark symmetry relations or lattice QCD. We use the calculations in Ref. [7] for $\bar{B} \to D\tau^-\bar{\nu}_\tau$ and in Ref. [8] for $\bar{B} \to D^*\tau^-\bar{\nu}_\tau$. For the $D^{**}(\ell/\tau)\nu$ background, we consider in the nominal fit only the four $L = 1$ states that have been measured [24]. We simulate these decays by using the Leibovich-Ligeti-Stewart-Wise calculation [25].

We validate and, when appropriate, correct the simulations by using three data control samples selected by one of the following criteria: $E_{\rm extra} > 0.5$ GeV [26], $q^2 \leq 4\,{\rm GeV}^2$, or $5.20 < m_{\rm ES} < 5.26$ GeV. We use off-peak data to correct the efficiency and the $|\boldsymbol{p}^*_\ell|$ spectrum of simulated continuum events. After this correction, the $m^2_{\rm miss}$ and $|\boldsymbol{p}^*_\ell|$ distributions of the background and normalization events agree very well with the simulation. However, we find that small differences in the $E_{\rm extra}$ spectrum and other BDT input distributions result in a 5%–10% efficiency difference between selected data and MC samples. We correct the continuum and $B\bar{B}$ backgrounds by using the $5.20 < m_{\rm ES} < 5.26$ GeV control sample. The same correction, with larger uncertainties, is applied to $D^{**}(\ell/\tau)\nu$ events, since their simulated $E_{\rm extra}$ spectrum is very similar.

We extract the signal and normalization yields from an extended, unbinned maximum-likelihood fit to two-dimensional $m^2_{\rm miss} - |\boldsymbol{p}^*_\ell|$ distributions. The fit is performed simultaneously to the four $D^{(*)}\ell$ samples and the four $D^{(*)}\pi^0\ell$ samples. The distribution of each $D^{(*)}\ell$ sample is described as the sum of eight contributions: $D\tau\nu$, $D^*\tau\nu$, $D\ell\nu$, $D^*\ell\nu$, $D^{**}(\ell/\tau)\nu$, charge cross-feed, other $B\bar{B}$, and continuum. The yields for the last three backgrounds are fixed in the fit to the expected values. A large fraction of $B \to D^*\ell\nu$ decays (for $B = B^0$ or B^+) is reconstructed in the $D\ell$ samples (feed-down). We leave those two contributions free in the fit and use the fitted yields to estimate the feed-down rate of $B \to D^*\tau\nu$ decays. Since $B \to D(\ell/\tau)\nu$ decays contributing to the $D^*\ell$ samples are rare, their rate is fixed to the expected value.

The four $D^{(*)}\pi^0\ell$ samples are described by six contributions: The $D^{(*)}\tau\nu$ and $D^{(*)}\ell\nu$ yields are combined, but otherwise the same contributions that describe the $D^{(*)}\ell$ samples are employed. The four $D^{**}(\ell/\tau)\nu$ yields in the control samples are free in the fit, but their ratios to the corresponding $D^{**}(\ell/\tau)\nu$ yields in the $D^{(*)}\ell$ samples are constrained to the expected values.

The fit relies on $8 \times 4 + 6 \times 4 = 56$ probability density functions (PDFs), which are determined from MC samples of continuum and $B\bar{B}$ events equivalent to 2 and 9 times the size of the data sample, respectively. The two-dimensional $m^2_{\rm miss} - |\boldsymbol{p}^*_\ell|$ distributions are described by using smooth nonparametric kernel estimators [27]. The fit is iterated to update some of the parameters that depend on the normalization yields, most importantly the rate of signal

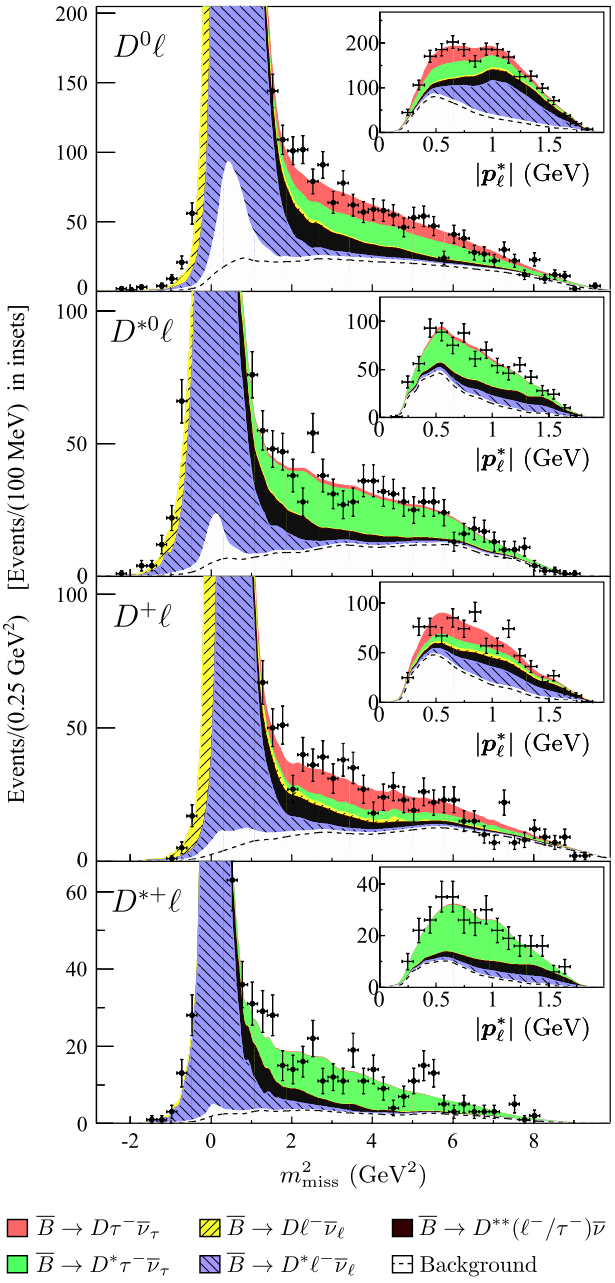

FIG. 1 (color online). Comparison of the data and the fit projections for the four $D^{(*)}\ell$ samples. The insets show the $|\boldsymbol{p}^*_\ell|$ projections for $m^2_{\rm miss} > 1$ GeV^2, which excludes most of the normalization modes. In the background component, the region above the dashed line corresponds to charge cross-feed, and the region below corresponds to continuum and $B\bar{B}$.

feed-down. This process converges after the first iteration. We performed MC studies to verify that neither the fit procedure nor the PDFs produced significant biases in the results.

Figure 1 shows the $m^2_{\rm miss}$ and $|\boldsymbol{p}^*_\ell|$ projections of the fit to the four $D^{(*)}\ell$ samples. The fit describes the data well, and the observed differences are consistent with the statistical and systematic uncertainties on the signal PDFs and background distributions.

We extract the branching fraction ratios as $\mathcal{R}(D^{(*)}) = (N_{\rm sig}/N_{\rm norm})/(\varepsilon_{\rm sig}/\varepsilon_{\rm norm})$, where $N_{\rm sig}$ and $N_{\rm norm}$ refer to the number of signal and normalization events, respectively, and $\varepsilon_{\rm sig}/\varepsilon_{\rm norm}$ is the ratio of their efficiencies derived from simulations. Table I shows the results of the fits for the four individual samples as well as an additional fit in which we impose the isospin relations $\mathcal{R}(D^0) = \mathcal{R}(D^+) \equiv \mathcal{R}(D)$ and $\mathcal{R}(D^{*0}) = \mathcal{R}(D^{*+}) \equiv \mathcal{R}(D^*)$. The statistical correlations are -0.59 for $\mathcal{R}(D^0)$ and $\mathcal{R}(D^{*0})$, -0.23 for $\mathcal{R}(D^+)$ and $\mathcal{R}(D^{*+})$, and -0.45 for $\mathcal{R}(D)$ and $\mathcal{R}(D^*)$. We have verified that the values of $\mathcal{R}(D^{(*)})$ from fits to samples corresponding to different run periods are consistent. We repeated the analysis, varying the selection criteria over a wide range corresponding to changes in the signal-to-background ratios between 0.3 and 1.3, and also arrive at consistent values of $\mathcal{R}(D^{(*)})$.

The largest systematic uncertainty affecting the fit results is due to the poorly understood $B \to D^{**}(\ell/\tau)\nu$ background. The PDFs that describe this contribution are impacted by the uncertainty on the branching fractions of the four $B \to D^{**}\ell\nu$ decays, the relative $\pi^0/\pi^\pm$ efficiency, and the branching fraction ratio of $B \to D^{**}\tau\nu$ to $B \to D^{**}\ell\nu$ decays. These effects contribute to an uncertainty of 2.1% on $\mathcal{R}(D)$ and 1.8% on $\mathcal{R}(D^*)$. We also repeated the fit including an additional floating component with the distributions of $B \to D^{(*)}\eta\ell\nu$, nonresonant $B \to D^{(*)}\pi(\pi)\ell\nu$, and $B \to D^{**}(\to D^{(*)}\pi\pi)\ell\nu$ decays. The $B \to D^{**}(\ell/\tau)\nu$ background is tightly constrained by the $D^{(*)}\pi^0\ell$ samples, and, as a result, all these fits yield similar values for $\mathcal{R}(D^{(*)})$. We assign the observed variation as a systematic uncertainty: 2.1% for $\mathcal{R}(D)$ and 2.6% for $\mathcal{R}(D^*)$.

We also account for the impact of the uncertainties described above on the relative efficiency of the $B \to D^{**}(\ell/\tau)\nu$ contributions to the signal and $D^{(*)}\pi^0\ell$ samples. In addition, the BDT selection introduces an uncertainty that we estimate as 100% of the efficiency correction that we determined from control samples. These effects result in uncertainties of 5.0% and 2.0% on $\mathcal{R}(D)$ and $\mathcal{R}(D^*)$, respectively.

The largest remaining uncertainties are due to the continuum and $B\bar{B}$ backgrounds [4.9% on $\mathcal{R}(D)$ and 2.7% on $\mathcal{R}(D^*)$] and the PDFs for the signal and normalization decays (4.3% and 2.1%). The uncertainties in the efficiency ratios $\varepsilon_{\rm sig}/\varepsilon_{\rm norm}$ are 2.6% and 1.6%; they do not affect the significance of the signal and are dominated by the limited size of the MC samples. Uncertainties due to the FFs, particle identification, final-state radiation, soft-pion reconstruction, and others related to the detector performance largely cancel in the ratio, contributing only about 1%. The individual systematic uncertainties are added in quadrature to define the total systematic uncertainty, reported in Table I.

There is a positive correlation between some of the systematic uncertainties on $\mathcal{R}(D)$ and $\mathcal{R}(D^*)$, and, as a result the correlation of the total uncertainties is reduced to -0.48 for $\mathcal{R}(D^0)$ and $\mathcal{R}(D^{*0})$, to -0.15 for $\mathcal{R}(D^+)$ and $\mathcal{R}(D^{*+})$, and to -0.27 for $\mathcal{R}(D)$ and $\mathcal{R}(D^*)$.

The statistical significance of the signal is determined as $\Sigma_{\rm stat} = \sqrt{2\Delta(\ln\mathcal{L})}$, where $\Delta(\ln\mathcal{L})$ is the change in the log-likelihood between the nominal fit and the no-signal hypothesis. The statistical and dominant systematic uncertainties are Gaussian. We estimate the overall significance as $\Sigma_{\rm tot} = \Sigma_{\rm stat} \times \sigma_{\rm stat}/\sqrt{\sigma^2_{\rm stat} + \sigma^{*2}_{\rm syst}}$, where $\sigma_{\rm stat}$ is the statistical uncertainty and $\sigma^*_{\rm syst}$ is the total systematic uncertainty affecting the fit. The significance of the $\bar{B} \to D\tau^-\bar{\nu}_\tau$ signal is 6.8σ, the first such measurement exceeding 5σ.

To compare the measured $\mathcal{R}(D^{(*)})$ with the SM predictions, we have updated the calculations in Refs. [8,31] taking into account recent FF measurements. Averaged over electrons and muons, we find $\mathcal{R}(D)_{\rm SM} = 0.297 \pm 0.017$ and $\mathcal{R}(D^*)_{\rm SM} = 0.252 \pm 0.003$. At this level of

TABLE I. Results of the isospin-unconstrained (top four rows) and isospin-constrained fits (last two rows). The columns show the signal and normalization yields, the ratio of their efficiencies, $\mathcal{R}(D^{(*)})$, branching fractions, and $\Sigma_{\rm stat}$ and $\Sigma_{\rm tot}$, the statistical and total significances, respectively. Where two uncertainties are given, the first is statistical and the second is systematic. The branching fractions $\mathcal{B}(\bar{B} \to D^{(*)}\tau^-\bar{\nu}_\tau)$ are calculated as $\mathcal{R}(D^{(*)}) \times \mathcal{B}(\bar{B} \to D^{(*)}\ell^-\bar{\nu}_\ell)$, by using the average $\bar{B} \to D^{(*)}\ell^-\bar{\nu}_\ell$ branching fractions measured by *BABAR* [28–30]. The stated branching fractions for the isospin-constrained fit refer to B^- decays.

Decay	$N_{\rm sig}$	$N_{\rm norm}$	$\varepsilon_{\rm sig}/\varepsilon_{\rm norm}$	$\mathcal{R}(D^{(*)})$	$\mathcal{B}(B \to D^{(*)}\tau\nu)(\%)$	$\Sigma_{\rm stat}$	$\Sigma_{\rm tot}$
$B^- \to D^0\tau^-\bar{\nu}_\tau$	314 ± 60	1995 ± 55	0.367 ± 0.011	$0.429 \pm 0.082 \pm 0.052$	$0.99 \pm 0.19 \pm 0.13$	5.5	4.7
$B^- \to D^{*0}\tau^-\bar{\nu}_\tau$	639 ± 62	8766 ± 104	0.227 ± 0.004	$0.322 \pm 0.032 \pm 0.022$	$1.71 \pm 0.17 \pm 0.13$	11.3	9.4
$\bar{B}^0 \to D^+\tau^-\bar{\nu}_\tau$	177 ± 31	986 ± 35	0.384 ± 0.014	$0.469 \pm 0.084 \pm 0.053$	$1.01 \pm 0.18 \pm 0.12$	6.1	5.2
$\bar{B}^0 \to D^{*+}\tau^-\bar{\nu}_\tau$	245 ± 27	3186 ± 61	0.217 ± 0.005	$0.355 \pm 0.039 \pm 0.021$	$1.74 \pm 0.19 \pm 0.12$	11.6	10.4
$\bar{B} \to D\tau^-\bar{\nu}_\tau$	489 ± 63	2981 ± 65	0.372 ± 0.010	$0.440 \pm 0.058 \pm 0.042$	$1.02 \pm 0.13 \pm 0.11$	8.4	6.8
$\bar{B} \to D^*\tau^-\bar{\nu}_\tau$	888 ± 63	11953 ± 122	0.224 ± 0.004	$0.332 \pm 0.024 \pm 0.018$	$1.76 \pm 0.13 \pm 0.12$	16.4	13.2

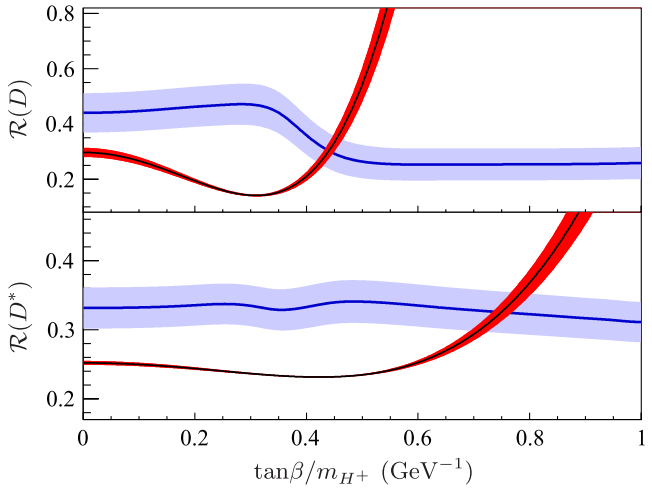

FIG. 2 (color online). Comparison of the results of this analysis (light gray, blue) with predictions that include a charged Higgs boson of type II 2HDM (dark gray, red). The SM corresponds to $\tan\beta/m_{H^+} = 0$.

precision, additional uncertainties could contribute [8], but the experimental uncertainties are expected to dominate.

Our measurements exceed the SM predictions for $\mathcal{R}(D)$ and $\mathcal{R}(D^*)$ by 2.0σ and 2.7σ, respectively. The combination of these results, including their -0.27 correlation, yields $\chi^2 = 14.6$ for 2 degrees of freedom, corresponding to a p value of 6.9×10^{-4}. Thus, the possibility of both the measured $\mathcal{R}(D)$ and $\mathcal{R}(D^*)$ agreeing with the SM predictions is excluded at the 3.4σ level [32].

Figure 2 shows the effect that a charged Higgs boson of the type II 2HDM [7,34] would have on $\mathcal{R}(D)$ and $\mathcal{R}(D^*)$ in terms of the ratio of the vacuum expectation values $\tan\beta \equiv v_2/v_1$ and the mass of the charged Higgs m_{H^+}. We estimate the effect of the 2HDM on our measurements by reweighting the simulated events at the matrix element level for 20 values of $\tan\beta/m_{H^+}$ over the $[0.05, 1]$ GeV^{-1} range. We then repeat the fit with updated PDF shapes and $\varepsilon_{\rm sig}/\varepsilon_{\rm norm}$ values. The increase in the uncertainty on the PDFs and the efficiency ratio is estimated for each value of $\tan\beta/m_{H^+}$. The other sources of systematic uncertainty are kept constant in relative terms.

The measured values of $\mathcal{R}(D)$ and $\mathcal{R}(D^*)$ match the predictions of this particular Higgs model for $\tan\beta/m_{H^+} = 0.44 \pm 0.02$ GeV^{-1} and $\tan\beta/m_{H^+} = 0.75 \pm 0.04$ GeV^{-1}, respectively. However, the combination of $\mathcal{R}(D)$ and $\mathcal{R}(D^*)$ excludes the type II 2HDM charged Higgs boson with a 99.8% confidence level for any value of $\tan\beta/m_{H^+}$. This calculation is valid only for values of m_{H^+} greater than about 10 GeV [4,7]. The region for $m_{H^+} \leq 10$ GeV has already been excluded by $B \to X_s\gamma$ measurements [35], and, therefore, the type II 2HDM is excluded in the full $\tan\beta - m_{H^+}$ parameter space.

In summary, we have measured the $\bar{B} \to D\tau^-\bar{\nu}_\tau$ and $\bar{B} \to D^*\tau^-\bar{\nu}_\tau$ decays relative to the decays to light leptons $\bar{B} \to D^{(*)}\ell^-\bar{\nu}_\ell$. We find

$$\mathcal{R}(D) = 0.440 \pm 0.058 \pm 0.042,$$
$$\mathcal{R}(D^*) = 0.332 \pm 0.024 \pm 0.018.$$

These results supersede the previous *BABAR* results and have significantly reduced uncertainties. The measured values are compatible with those measured by the Belle Collaboration [12,14,15].

The results presented here disagree with the SM at the 3.4σ level, which, together with the measurements by the Belle Collaboration, could be an indication of new physics processes affecting $\bar{B} \to D^{(*)}\tau^-\bar{\nu}_\tau$ decays. However, our results are not compatible with the widely discussed type II 2HDM for any value of $\tan\beta$ and m_{H^+}.

We acknowledge M. Mazur for his help throughout the analysis and S. Westhoff, S. Fajfer, J. Kamenik, and I. Nišandžić for their help with the calculation of the charged Higgs contributions. We are grateful for the excellent luminosity and machine conditions provided by our PEP-II colleagues and for the substantial dedicated effort from the computing organizations that support *BABAR*. The collaborating institutions thank SLAC for its support and kind hospitality. This work is supported by DOE and NSF (USA), NSERC (Canada), CEA and CNRS-IN2P3 (France), BMBF and DFG (Germany), INFN (Italy), FOM (Netherlands), NFR (Norway), MES (Russia), MICIIN (Spain), and STFC (United Kingdom). Individuals have received support from the Marie Curie EIF (European Union) and the A. P. Sloan Foundation (USA).

*Now at the University of Tabuk, Tabuk 71491, Saudi Arabia.
†Also with Università di Perugia, Dipartimento di Fisica, Perugia, Italy.
‡Now at the University of Huddersfield, Huddersfield HD1 3DH, United Kingdom.
§Now at University of South Alabama, Mobile, AL 36688, USA.
‖Also with Università di Sassari, Sassari, Italy.
¶Deceased.

[1] P. Heiliger and L. Sehgal, Phys. Lett. B **229**, 409 (1989).
[2] J. G. Korner and G. A. Schuler, Z. Phys. C **46**, 93 (1990).
[3] D. S. Hwang and D. W. Kim, Eur. Phys. J. C **14**, 271 (2000).
[4] M. Tanaka, Z. Phys. C **67**, 321 (1995).
[5] H. Itoh, S. Komine, and Y. Okada, Prog. Theor. Phys. **114**, 179 (2005).
[6] U. Nierste, S. Trine, and S. Westhoff, Phys. Rev. D **78**, 015006 (2008).
[7] M. Tanaka and R. Watanabe, Phys. Rev. D **82**, 034027 (2010).
[8] S. Fajfer, J. F. Kamenik, and I. Nišandžić, Phys. Rev. D **85**, 094025 (2012).

[9] Throughout this Letter, ℓ refers only to the light leptons e and μ, $D^{(*)}$ refers to a D or a D^* meson, and charge-conjugate decay modes are implied.
[10] M. Antonelli *et al.*, Phys. Rep. **494**, 197 (2010).
[11] K. Nakamura *et al.* (Particle Data Group), J. Phys. G **37**, 075021 (2010).
[12] A. Matyja *et al.* (Belle Collaboration), Phys. Rev. Lett. **99**, 191807 (2007).
[13] B. Aubert *et al.* (*BABAR* Collaboration), Phys. Rev. Lett. **100**, 021801 (2008).
[14] I. Adachi *et al.* (Belle Collaboration), arXiv:0910.4301.
[15] A. Bozek *et al.* (Belle Collaboration), Phys. Rev. D **82**, 072005 (2010).
[16] B. Aubert *et al.* (*BABAR* Collaboration), Nucl. Instrum. Methods Phys. Res., Sect. A **479**, 1 (2002).
[17] B. Aubert *et al.* (*BABAR* Collaboration), Phys. Rev. Lett. **92**, 071802 (2004).
[18] A. Hoecker *et al.*, 2010, MVA Toolkit for Multivariate Data Analysis with ROOT, http://tmva.sourceforge.net.
[19] T. Sjostrand, Comput. Phys. Commun. **82**, 74 (1994).
[20] D. Lange, Nucl. Instrum. Methods Phys. Res., Sect. A **462**, 152 (2001).
[21] S. Agostinelli *et al.* (GEANT4 Collaboration), Nucl. Instrum. Methods Phys. Res., Sect. A **506**, 250 (2003).
[22] I. Caprini, L. Lellouch, and M. Neubert, Nucl. Phys. **B530**, 153 (1998).
[23] Y. Amhis *et al.* (Heavy Flavor Averaging Group Collaboration), arXiv:1207.1158.
[24] B. Aubert *et al.* (*BABAR* Collaboration), Phys. Rev. Lett. **101**, 261802 (2008).
[25] A. K. Leibovich, Z. Ligeti, I. W. Stewart, and M. B. Wise, Phys. Rev. D **57**, 308 (1998).
[26] We do not place explicit requirements on $E_{\rm extra}$, but the BDTs reject all events with $E_{\rm extra} > 0.4$ GeV.
[27] K. S. Cranmer, Comput. Phys. Commun. **136**, 198 (2001).
[28] B. Aubert *et al.* (*BABAR* Collaboration), Phys. Rev. Lett. **104**, 011802 (2010).
[29] B. Aubert *et al.* (*BABAR* Collaboration), Phys. Rev. D **79**, 012002 (2009).
[30] B. Aubert *et al.* (*BABAR* Collaboration), Phys. Rev. D **77**, 032002 (2008).
[31] J. F. Kamenik and F. Mescia, Phys. Rev. D **78**, 014003 (2008).
[32] Recent calculations [6,7,33] have found values of $\mathcal{R}(D)_{\rm SM}$ that somewhat exceed our estimation. With the largest of those values, the significance of the excess decreases to 3.2σ.
[33] J. A. Bailey *et al.*, Phys. Rev. Lett. **109**, 071802 (2012).
[34] V. D. Barger, J. Hewett, and R. Phillips, Phys. Rev. D **41**, 3421 (1990).
[35] M. Misiak *et al.*, Phys. Rev. Lett. **98**, 022002 (2007).